Modeling Oxygen Transport into Different Parts of a PET Bottle Containing Water Stored at Various Temperatures

Wannaporn Kaewboonruang[1], Kuson Bawornruttanaboonya[2], Tipaporn Yoovidhya[3*] and Sakamon Devahastin[4]

King Mongkut's University of Technology Thonburi, Bandmod, Thungkru, Bangkok 10140

Abstract

A diffusion-based model, in conjunction with Henry's law to treat an interface equilibrium, is proposed to predict oxygen transport through a PET bottle containing water stored at various temperatures. The model was validated against the experimental oxygen concentration evolutions in the headspace and water regions and noted to provide adequate prediction. Simulation revealed that oxygen transport through a PP cap was 90-96% and that through the PET body was 73-92% of the total oxygen transport into the headspace and water regions, respectively. Simulation also revealed that the traditional way of reporting oxygen transport rate per unit area may result in misleading behavior of oxygen transport through various parts of a bottle. Decreased bottle thickness (from 0.3 to 0.1 mm) resulted in a higher dissolved oxygen concentration, while type of cap material (PP and PET) did not pose any significant effect, especially during the first 20 days of storage.

Keywords : Diffusion / Dissolved Oxygen / Headspace / Mass Transfer / Mathematical Modeling / Oxygen Permeability

* *Corresponding Author : tipaporn.yoo@kmutt.ac.th*

[1] *Graduate Student, Advanced Food Processing Research Laboratory, Department of Food Engineering, Faculty of Engineering.*

[2] *Graduate Student, Advanced Food Processing Research Laboratory, Department of Food Engineering, Faculty of Engineering.*

[3] *Associate Professor, Advanced Food Processing Research Laboratory, Department of Food Engineering, Faculty of Engineering.*

[4] *Professor, Advanced Food Processing Research Laboratory, Department of Food Engineering, Faculty of Engineering.*

การจำลองการถ่ายเทออกซิเจนเข้าสู่บริเวณต่างๆ ของขวด PET ที่บรรจุน้ำและเก็บรักษาที่อุณหภูมิต่าง ๆ

วรรณพร แก้วบุญเรือง[1] กุศล บวรรัตนบุญญา[2] ทิพาพร อยู่วิทยา[3*] และ สักกมน เทพหัสดิน ณ อยุธยา[4]

มหาวิทยาลัยเทคโนโลยีพระจอมเกล้าธนบุรี แขวงบางมด เขตทุ่งครุ กรุงเทพฯ 10140

บทคัดย่อ

งานวิจัยนี้เป็นการประยุกต์ใช้แบบจำลองที่พัฒนาขึ้นบนพื้นฐานของการแพร่ร่วมกับกฎของ Henry (Henry's law) เพื่ออธิบายสภาวะสมดุลที่ขอบเขตของวัฏภาคน้ำและช่องว่างเหนือน้ำเพื่อทำนายพฤติกรรมการถ่ายเทออกซิเจนผ่านบริเวณต่าง ๆ ของขวดพลาสติกชนิด PET ที่บรรจุน้ำ และเก็บรักษาไว้ที่อุณหภูมิต่าง ๆ ทั้งนี้เมื่อทวนสอบความแม่นยำของแบบจำลองกับข้อมูลผลการทดลองการเปลี่ยนแปลงความเข้มข้นของออกซิเจนทั้งในบริเวณช่องว่างเหนือน้ำและในน้ำ พบว่าแบบจำลองสามารถทำนายผลได้เป็นที่น่าพอใจ ผลการจำลองแสดงให้เห็นว่าออกซิเจนถ่ายเทผ่านบริเวณฝาขวดคิดเป็นร้อยละ 90-96 และผ่านบริเวณตัวขวด PET คิดเป็นร้อยละ 73-92 ของออกซิเจนทั้งหมดที่ถ่ายเทเข้าสู่บริเวณช่องว่างเหนือน้ำและที่ละลายในน้ำ ตามลำดับ นอกจากนี้ผลการจำลองยังแสดงให้เห็นว่าวิธีดั้งเดิมที่ใช้ในการวิเคราะห์ข้อมูลการถ่ายเทออกซิเจนที่คำนวณออกมาในรูปของอัตราการถ่ายเทออกซิเจนต่อหน่วยพื้นที่การถ่ายเท อาจทำให้เกิดความเข้าใจผิดเกี่ยวกับพฤติกรรมการถ่ายเทออกซิเจนผ่านบริเวณต่าง ๆ ของขวด และเมื่อใช้แบบจำลองในการพิจารณาผลของความหนาของขวด โดยลดความหนาของขวดลงจาก 0.3 เป็น 0.1 มิลลิเมตรจะทำให้ความเข้มข้นของออกซิเจนที่ละลายในน้ำสูงขึ้น ในขณะที่ชนิดของวัสดุที่ใช้ผลิตฝาไม่ส่งผลกระทบอย่างมีนัยสำคัญต่อความเข้มข้นดังกล่าว โดยเฉพาะอย่างยิ่งในช่วง 20 วันแรกของการเก็บรักษา

คำสำคัญ : การแพร่ / ออกซิเจนที่ละลายในน้ำ / ช่องว่างเหนือน้ำ / การถ่ายโอนมวล / แบบจำลองทางคณิตศาสตร์ / การซึมผ่านออกซิเจน

* *Corresponding Author : tipaporn.yoo@kmutt.ac.th*

[1] *นักศึกษาปริญญาโท ห้องปฏิบัติการแปรรูปอาหารขั้นสูง ภาควิชาวิศวกรรมอาหาร คณะวิศวกรรมศาสตร์*

[2] *นักศึกษาปริญญาเอก ห้องปฏิบัติการแปรรูปอาหารขั้นสูง ภาควิชาวิศวกรรมอาหาร คณะวิศวกรรมศาสตร์*

[3] *รองศาสตราจารย์ ห้องปฏิบัติการแปรรูปอาหารขั้นสูง ภาควิชาวิศวกรรมอาหาร คณะวิศวกรรมศาสตร์*

[4] *ศาสตราจารย์ ห้องปฏิบัติการแปรรูปอาหารขั้นสูง ภาควิชาวิศวกรรมอาหาร คณะวิศวกรรมศาสตร์*

1. Introduction

Information on oxygen transport through food packagings is of great importance as oxygen can lead to many such adverse changes as oxidation reactions and losses of bioactive compounds and hence the lower product quality and shorter shelf life [1-4]. Oxygen transport through packagings depends on a number of parameters, including the packaging structure, packaging thickness as well as storage temperature and difference in the partial pressure of oxygen within and outside of the packagings [5-6].

For many beverages, polyethylene terephthalate (PET) is used as a body of a bottle, while polypropylene (PP) is used as a cap. Due to the different oxygen permeabilities, these materials allow oxygen to pass through their bodies at different rates. Nevertheless, oxygen can migrate from one portion to another, e.g., from the headspace region to the beverage region. In order to minimize the transport of oxygen into packaged beverage, it is important to understand the behavior of oxygen transport through various parts of a beverage bottle; oxygen transport through an interface between the headspace and beverage regions also needs to be considered. Storage temperature also plays an important role in the oxygen transport behavior and must be taken into account in the analysis. Since an experimental program to understand such a transport behavior would be complicated and time consuming, use of a reliable mathematical model is an interesting alternative.

Many studies have attempted to model oxygen transport through various food packagings. Di Felice et al. [7], for example, studied the gas permeation rate through plastic packaging walls and developed a model to predict the gas concentration in a water-filled bottle. However, the developed model considered only the oxygen permeation through the bottle walls into the liquid and did not take into account the thickness of the bottle, which is one of the factors affecting the transmission of oxygen. Van Bree et al. [8] proposed an approach to predict the concentration of oxygen that transported into the headspace of various packagings. The effect of packaging thickness was also considered. No attempt was made to distinguish between the oxygen transported into the bottle via its body and its cap, however. More recently, Bacigalupi et al. [9] presented a model for studying the transfer of oxygen, which resulted in ascorbic acid oxidation of orange juice in a PET bottle. The results showed that the oxygen transport through the cap was an important issue. However, the model considered only the oxygen migration into the beverage and not to the headspace. Transport between those two regions through an interface was not considered.

Although a number of models are available to study the transport of oxygen through a PET bottle, no model considers the simultaneous transport of oxygen to both the headspace and beverage regions. No study also exists on the effect of oxygen transport through a headspace-beverage interface. Use of an appropriate model to perform a parametric study on the effects of the bottle thickness and cap material on the oxygen transport behavior and the evolution of the concentration of oxygen dissolved in a beverage is also lacking.

In this work, a mathematical model based on Fick's law of diffusion in conjunction with Henry's law to treat an interface equilibrium is proposed. The model was first validated with our own data on the evolution of the oxygen concentration in both headspace and beverage regions. Water was used as a model beverage to avoid the possible alteration of the oxygen transport behavior as a result of the oxidation reactions that may take place should a real beverage, which normally contains oxygen-sensitive

ingredients, was used. The model was then used to numerically investigate the OTR through a PET bottle body and cap at different storage temperatures. Oxygen transport within the bottle, i.e., transport between the headspace and water regions through an interface, was also investigated. The model was eventually used to study the effects of bottle thickness and cap material on the amount of oxygen transported into the water and also on the evolution of the dissolved oxygen concentration in the water.

2. Materials and methods

2.1 PET bottles

Preformed PET bottles with PCO-1810 neck finishes were purchased from Precision Plastic Co., Ltd. (Ayutthaya, Thailand). They were blown by a blow molding machine (SIDEL, SBO 20, Octeville-sur-Mer, France) to the following dimensions: diameter of 69.3 mm, height of 207 mm and thickness of 0.3 mm (see Fig. 1).

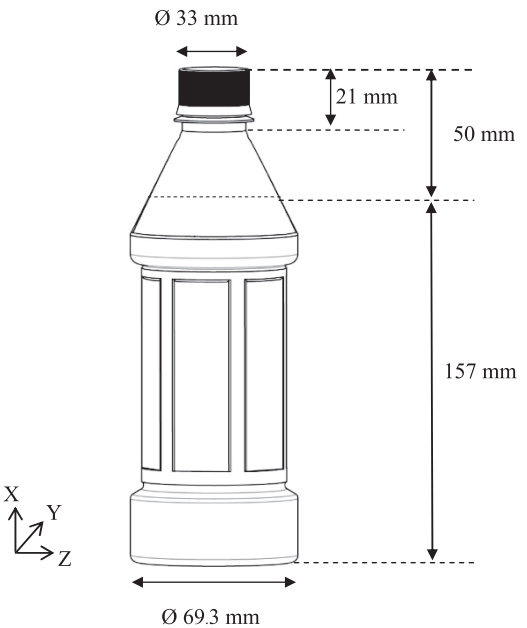

Figure 1 Schematic diagram of simulated PET bottle

2.2 Chemical

Manganese sulfate monohydrate ($MnSO_4 \cdot H_2O$), sodium hydroxide (NaOH), potassium iodide (KI) and sulfuric acid were purchased from Carlo Erba (Milan, Italy). Sodium thiosulfate ($Na_2S_2O_3 \cdot 5H_2O$) and soluble starch were purchased from Carlo Erba (Rodano, MI). Salicylic acid was purchased from May and Baker (London, UK).

2.3 Bottled water preparation

A bottle was first rinsed with hot water. Fresh water was sterilized at 135 °C using a sterilizer (Integra, 14050/ PS-137190/ A-R, Samutprakarn, Thailand). The water was filled into the bottle at a temperature of around 90 °C by a filler (BC Technology, Magic HF, Cuggiono, Italy). After capping via the use of a capper (AROL, TSI-EURO PK "L.E.S", Canelli, Italy), the bottle and its content was cooled in a cooling tunnel (FMI, C33-168-1, Milan, Italy) to the final product temperature of around 35-37 °C. Bottled water was stored at 35, 45 and 55 °C in three different incubators (Memmert, BE 500 Incubator, Schwabach, Germany); the storage temperatures of 35 and 45 °C refer to the typical warehouse storage temperature in Thailand, while the storage temperatures of 55 °C refers to the shipping temperature from Thailand to some Middle East and African countries.

2.4 Determination of headspace oxygen concentration

Three water-filled bottles stored at each temperature were taken out for the analysis at every 5 days over a period of 60 days, then every 10 days until 100 days. Each bottle was punctured at its shoulder with a needle of 0.55 mm in diameter and 25 mm in length to measure the oxygen concentration in the headspace by using a portable

gas analyzer (Checkpoint, PBI Dansensor®, Ringsted, Denmark) with an accuracy of ±0.102 mol m^{-3}. A septum was used to seal the needle to avoid leakage of oxygen. The oxygen concentration at each sampling time is reported as an average of the values in the three bottles.

2.5 Determination of dissolved oxygen concentration

Dissolved oxygen concentration was determined by the Winkler method. The detail of the method was given by Balance et al. [10]. The water-filled bottles stored at each temperature were taken out for the analysis at every 5 days over a period of 60 days, then every 10 days until 100 days.

2.6 Determination of oxygen permeability of PET

Oxygen permeability was calculated from the OTR as shown in Eq. (1). OTR was in turn measured as per the ASTM F 1307-02 method [11] using a coulometric sensor (Illinois Instruments, Oxygen Permeation Analyzer 8001, Johnsburg, IL) at 35±2, 45±2 and 55±2 °C and 65±5% relative humidity. OTR was determined when the bottle had reached an equilibrium with the test environment. The determination of OTR was conducted by the Thailand Institute of Scientific and Technological Research (TISTR).

$$\text{Oxygen permeability } (\text{mol m}^{-1}\text{s}^{-1}\text{Pa}^{-1}) = \frac{\text{OTR } (\text{mol m}^{-2}\text{s}^{-1}) \times \text{Thickness (m)}}{\text{Partial pressure difference of oxygen across the bottle (Pa)}} \quad (1)$$

3. Mathematical model development

3.1 Geometry construction

The geometry and dimensions of the simulated bottle are shown in Fig. 1. The total volume and surface area of the bottle as determined via the use of SolidWorks 2014 (Dassault Systèmes SolidWorks Corp., Waltham, MA) are 350 cm^3 and 445.5 cm^2, respectively. The bottle is made of PET, while the cap is made of PP.

3.2 Model assumptions

To simplify the analysis, the following assumptions were made:

- Oxygen diffusivity is constant at a given temperature.
- Time required for the water temperature to reach the storage temperature is negligible when compared with the total storage time. The energy equation is therefore not required.
- Volume of both phases (water and headspace) are constant.
- Temperature is constant during the whole storage period.
- Bottle thickness is uniform.
- No flow and chemical reaction take place within the bottle.

3.3 Oxygen transport model

3.3.1 Model equations

The oxygen transport from the surrounding through the bottle wall and cap into the headspace and water regions was modeled using the following oxygen balance equations:

Headspace region:

$$\left(\frac{\partial C_{O_2}}{\partial t}\right) = D_{O_2}\left(\frac{\partial^2 C_{O_2}}{\partial x^2} + \frac{\partial^2 C_{O_2}}{\partial y^2} + \frac{\partial^2 C_{O_2}}{\partial z^2}\right) \quad (2)$$

Water region:

$$\left(\frac{\partial C'_{O_2}}{\partial t}\right) = D'_{O_2}\left(\frac{\partial^2 C'_{O_2}}{\partial x^2} + \frac{\partial^2 C'_{O_2}}{\partial y^2} + \frac{\partial^2 C'_{O_2}}{\partial z^2}\right) \quad (3)$$

where C_{O_2} is the molar concentration of oxygen in the headspace region (mol m^{-3}), C'_{O_2} is the molar concentration of dissolved oxygen in the water (mol m^{-3}), D_{O_2} is the diffusion coefficient of oxygen through air in the headspace region (m^2 s^{-1}) and D'_{O_2} is the diffusion coefficient of oxygen in the water ($m^2 s^{-1}$).

3.3.2 Initial and boundary conditions

The initial oxygen concentrations at the three storage temperatures, which were experimentally determined as per the method outlined in Sections 2.4 and 2.5, as well as the boundary conditions needed to solve Eqs. (2) and (3) are as follows:

Initial conditions (at *t*=0):

- *T* = 35 °C:
  C_{O_2} = 8.00 mol m^{-3}
  C'_{O_2} = 0.12 mol m^{-3}
- *T* = 45 °C:
  C_{O_2} = 7.98 mol m^{-3}
  C_{O_2} = 0.13 mol m^{-3}
- *T* = 55 °C:
  C_{O_2} = 7.88 mol m^{-3}
  C'_{O_2} = 0.13 mol m^{-3}

Boundary conditions [9]:

- Headspace region:

Oxygen transport through the PP cap and PET bottle surrounded the headspace region into the headspace is described by Eq. (4). The external partial pressures of oxygen ($p_{O_{2,out}}$) was set to be the partial pressure of oxygen in air, while the internal partial pressure of oxygen ($p_{O_{2,in}}$) is expressed in Eq. (5). The final equation for the oxygen flux through the headspace region therefore becomes Eq. (6).

$$J_{O_2} = \frac{U}{x}\left(p_{O_{2,out}} - p_{O_{2,in}}\right) \quad (4)$$

$$p_{O_{2,in}} = P_{total}\frac{C_{O_2}MW_{air}}{\rho_{air}} \quad (5)$$

$$J_{O_2} = \frac{U}{x}\left(p_{O_{2,out}} - P_{total}\frac{C_{O_2}MW_{air}}{\rho_{air}}\right) \quad (6)$$

where J_{O_2} is the total molar flux of oxygen to the headspace region (mol m^{-2} s^{-1}); *U* is the oxygen permeability of the bottle (mol m^{-1} s^{-1} Pa^{-1}); x is the bottle thickness (mm); $p_{O_{2,out}}$ and $p_{O_{2,in}}$ are the external and internal partial pressures of oxygen (Pa), respectively; P_{total} is the total pressure in the bottle (Pa); C_{O_2} is the molar concentration of oxygen in the headspace region (mol m^{-3}); MW_{air} is the molecular weight of air (kg mol^{-1}) and ρ_{air} is the density of air (kg m^{-3}).

Water region:

Oxygen flux through the PET bottle surrounded the water region into the water is described in Eq. (7).

$$J'_{O_2} = \frac{U}{x}\left(p_{O_{2,out}} - \frac{C'_{O_2}}{S_{O_2}}\right) \quad (7)$$

where J'_{O_2} is the total molar flux of oxygen into the water (mol m^{-2} s^{-1}); C'_{O_2} is the molar concentration of oxygen in the water (mol m^{-3}) and S_{O_2} is the

oxygen solubility in the water (mol m^{-3} Pa^{-1}) which is the Henry's law constant for the dissolution of oxygen into water.

$$C'_{O_2} = S_{O_2} \times p_{O_{2,in}} \quad (8)$$

where C'_{O_2} is the molar concentration of oxygen in the water (mol m^{-3}), $p_{O_{2,in}}$ is partial pressures of oxygen over headspace region (Pa) and S_{O_2} is the oxygen solubility in the water (mol m^{-3} Pa^{-1}).

The boundary conditions are summarized as shown in Fig. 2, while all the parameters used in the simulation are listed in Table 1.

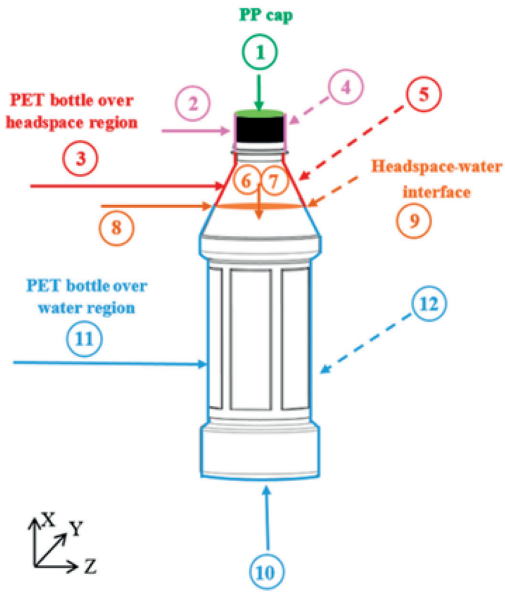

Region	Coordinate direction	No. of variable	Equation
Headspace	x	1	$J_{O_2} = \frac{U}{x}\left(p_{O_{2,out}} - P_{total}\frac{C_{O_2}MW_{air}}{\rho_{air}}\right)$
	y	2	$\frac{\partial C_{O_2}}{\partial y} = 0$
		3	$J_{O_2} = \frac{U}{x}\left(p_{O_{2,out}} - P_{total}\frac{C_{O_2}MW_{air}}{\rho_{air}}\right)$
	z	4	$\frac{\partial C_{O_2}}{\partial z} = 0$
		5	$J_{O_2} = \frac{U}{x}\left(p_{O_{2,out}} - P_{total}\frac{C_{O_2}MW_{air}}{\rho_{air}}\right)$
Interface	x	6-7	$C'_{O_2} = S_{O_2} \times P_{total}\frac{C_{O_2}MW_{air}}{\rho_{air}}$
	y	8	$\frac{\partial C'_{O_2}}{\partial y} = 0$
	z	9	$\frac{\partial C'_{O_2}}{\partial z} = 0$
Water	x	10	$J'_{O_2} = \frac{P}{x}\left(p_{O_{2,out}} - \frac{C'_{O_2}}{S_{O_2}}\right)$
	y	11	$J'_{O_2} = \frac{P}{x}\left(p_{O_{2,out}} - \frac{C'_{O_2}}{S_{O_2}}\right)$
	z	12	$J'_{O_2} = \frac{P}{x}\left(p_{O_{2,out}} - \frac{C'_{O_2}}{S_{O_2}}\right)$

Figure 2 Expressions of oxygen fluxes at various locations

Table 1 Parameters used in the simulation

Parameter	Value	Source
Partial pressure of oxygen outside bottle ($p_{O_{2,out}}$, Pa)	2.13×10^4	This work
Total pressure within bottle (P_{total}, Pa)	7.80×10^4	This work
Molecular weight of air (MW_{air}, g mol^{-1})	28.96	[14]
Molecular weight of oxygen (MW_{O_2}, g mol^{-1})	32.00	[14]

Table 1 Parameters used in the simulation (cont'd)

Parameter	Value	Source
Density of air at 35 °C (ρ_{air}, g m^{-3})	1.15×10^{3}	[15]
Density of air at 45 °C (ρ_{air}, g m^{-3})	1.11×10^{3}	[15]
Density of air at 55 °C (ρ_{air}, g m^{-3})	1.08×10^{3}	[15]
Density of oxygen at 35 °C (ρ_{O_2}, g m^{-3})	1.26×10^{3}	[16]
Density of oxygen at 45 °C (ρ_{O_2}, g m^{-3})	1.22×10^{3}	[16]
Density of oxygen at 55 °C (ρ_{O_2}, g m^{-3})	1.18×10^{3}	[16]
Oxygen permeability of PET at 35 °C ($U_{PET,35}$, mol m^{-1} s^{-1} Pa^{-1})	1.17×10^{-17}	This work
Oxygen permeability of PET at 45 °C ($U_{PET,45}$, mol m^{-1} s^{-1} Pa^{-1})	1.59×10^{-17}	This work
Oxygen permeability of PET at 55 °C ($U_{PET,55}$, mol m^{-1} s^{-1} Pa^{-1})	2.01×10^{-17}	This work
Oxygen permeability of PP at 35 °C ($U_{PP,35}$, , mol m^{-1} s^{-1} Pa^{-1})	2.20×10^{-15}	This work
Oxygen permeability of PP at 45 °C ($U_{PP,45}$, mol m^{-1} s^{-1} Pa^{-1})	5.10×10^{-15}	This work
Oxygen permeability of PP at 55 °C ($U_{PP,55}$, mol m^{-1} s^{-1} Pa^{-1})	1.12×10^{-14}	This work
Oxygen solubility in water at 35 °C (S_{35}, mol m^{-3} Pa^{-1})	1.07×10^{-5}	[13]
Oxygen solubility in water at 45 °C (S_{45}, mol m^{-3} Pa^{-1})	8.96×10^{-6}	[13]
Oxygen solubility in water at 55 °C (S_{55}, mol m^{-3} Pa^{-1})	7.61×10^{-6}	[13]
Oxygen diffusion coefficient in air at 35 °C (D_{35}, m^2 s^{-1})	2.21×10^{-5}	[17]
Oxygen diffusion coefficient in air at 45 °C (D_{45}, m^2 s^{-1})	2.33×10^{-5}	[17]
Oxygen diffusion coefficient in air at 55 °C (D_{55}, m^2 s^{-1})	2.45×10^{-5}	[17]
Oxygen diffusion coefficient in water at 35 °C (D'_{35}, m^2 s^{-1})	2.95×10^{-9}	[16]
Oxygen diffusion coefficient in water at 45 °C (D'_{45}, m^2 s^{-1})	3.65×10^{-9}	[16]
Oxygen diffusion coefficient in water at 55 °C (D'_{55}, m^2 s^{-1})	4.35×10^{-9}	[16]

3.4 Model implementation

The model equations, along with the initial and boundary conditions, were solved using the finite element method through COMSOL Multiphysics™ version 5.0 (Comsol AB, Stockholm, Sweden). The bottle geometry was drawn by SolidWorks 2014 and then imported into the COMSOL Multiphysics™ software as shown in Fig. 3.

Different mesh elements were tested to obtain mesh-independent solutions. The differences in the average oxygen concentration in both the headspace and water regions between using 43,892 and 182,993 elements were negligible. Mesh distribution within the bottle is as shown in Fig. 4. Different time steps (60 vs. 86,400 s) were also tested and the time step of 86,400 s (1 day) were noted to be adequate to simulate the oxygen transport process. Therefore, 43,892 elements and 86,400 s were used in all the simulations.

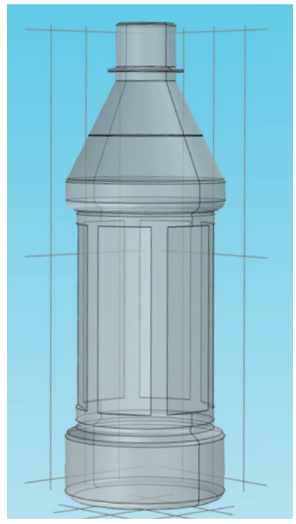

Figure 3 Model geometry of simulated PET bottle

Figure 4 Mesh distribution within the PET bottle

3.5 OTR calculation from the simulated fluxes of oxygen

OTR was calculated from the simulated fluxes of oxygen through different regions (PP cap, PET bottle over headspace region, PET bottle over water region and headspace-water interface) of the water bottle as shown in Eq. (9).

$$\mathrm{OTR}\ (\mathrm{cm^3 m^{-2} Day^{-1}}) = \frac{\text{Oxygen flux}\left(\mathrm{mol\ m^{-2} s^{-1}}\right) \times \mathrm{MW_{O_2}}\left(\mathrm{g\ mol^{-1}}\right) \times 86400\ (\mathrm{s\ day^{-1}})}{\text{Density of oxygen}(\mathrm{g\ cm^{-3}})} \quad \textbf{(9)}$$

4. Results and discussion

4.1 Oxygen permeability

In this study, the oxygen permeability of an empty PET bottle (with no cap) are noted to be 1.17×10^{-17}, 1.59×10^{-17} and 2.01×10^{-17} mol m^{-1} s^{-1} Pa^{-1} at 35, 45 and 55 °C, respectively. These values are similar to those reported by Schmid et al. [18], which are 1.23×10^{-17}, 2.01×10^{-17} and 2.93×10^{-17} mol m^{-1} s^{-1} Pa^{-1} at 35, 45 and 55 °C, respectively.

4.2 Experimental evolution of oxygen concentrations

The volumes of the headspace and water regions of the bottle are 30 cm^3 and 320 cm^3, respectively. The initial concentrations of oxygen in the headspace region at 35, 45 and 55 °C were 8.00, 7.98 and 7.88 mol m^{-3}, respectively; the initial concentrations of the dissolved oxygen in water at 35, 45 and 55 °C were measured to be 0.116, 0.133 and 0.134 mol m^{-3}, respectively.

The oxygen concentration in the headspace region continuously increased during 100 days of storage at all temperatures as is seen in Fig. 5a; the final concentrations were 9.18, 9.43 and 9.96 mol m^{-3} at 35, 45 and 55 °C, respectively. The higher oxygen concentration at a higher storage temperature is due to the higher oxygen permeability of PET.

The dissolved oxygen concentration in the water region (Fig. 5b) at 35 °C continuously increased until 60 days and then remained almost unchanged up to 100 days of storage. Similar trends were observed at 45 and 55 °C. The final dissolved oxygen concentrations reached 0.207, 0.187 and 0.167 mol m^{-3} at 35, 45 and 55 °C, respectively. The final concentrations at all temperatures were close to the saturation concentrations of oxygen in water, which are 0.217, 0.185 and 0.159 mol m^{-3}, respectively [19]. Oxygen solubility decreases as the storage temperature increases, resulting in a lower dissolved oxygen concentration [20, 21].

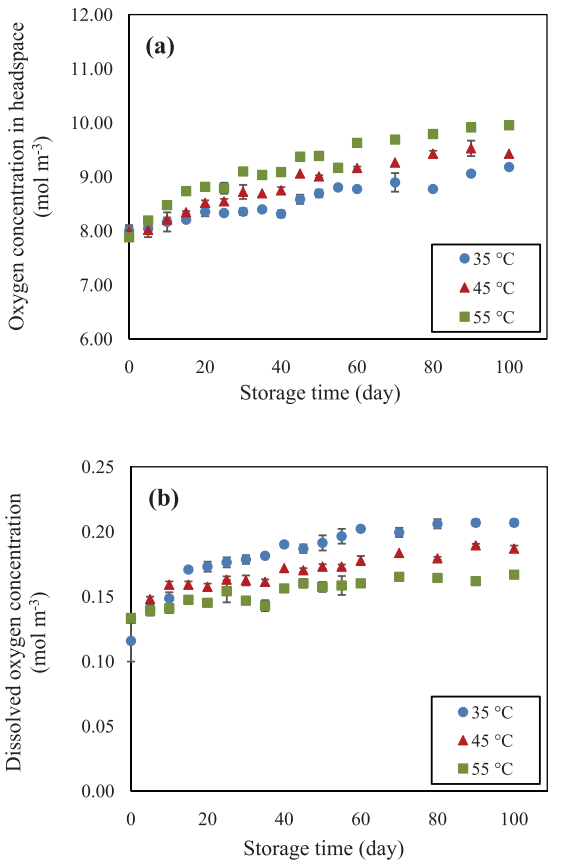

Figure 5 Experimental evolutions of (a) oxygen concentration in headspace and (b) dissolved oxygen concentration

4.3 Modeling of oxygen transport behavior

Fig. 6 shows a comparison between the experimental and predicted oxygen concentration evolutions in the headspace region. The oxygen permeability value of PP was obtained by fitting the simulated results to the experimental data at each temperature as shown in Table 1. The model was able to adequately predict the oxygen concentration evolutions in the headspace region at all storage temperatures with R^2 = 0.91, 0.97 and 0.96 at the storage temperatures of 35 and 45, 55 °C, respectively.

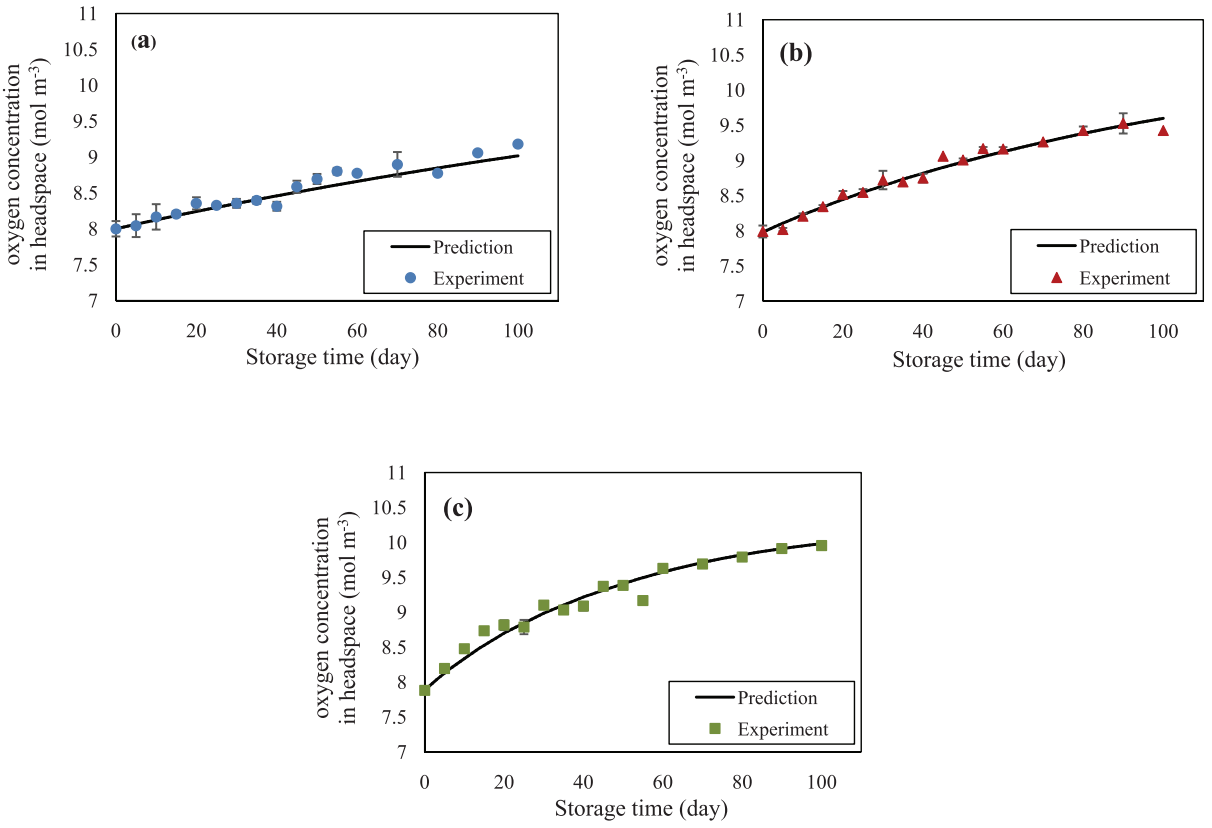

Figure 6 Experimental and predicted oxygen concentration evolutions in headspace at (a) 35 °C; (b) 45 °C and (c) 55 °C

For the prediction of the dissolved oxygen concentration evolution, the predictability of the model with and without the consideration of the oxygen transport through the headspace-water interface was first compared; better prediction with the consideration of the headspace-water interface, especially at a lower storage temperature, is seen as shown in Fig. 7. This is because the transport of oxygen was limited by the solubility of oxygen in water as per the Henry's law; the effect was felt more at a higher temperature due to the lower oxygen solubility in water. Therefore, the headspace-water interface is a very important boundary condition that should always be considered when

attempting to predict the evolution of the concentration of oxygen, which could transport from the other region of the bottle into the water. R^2 of the predicted dissolve oxygen concentration at the storage temperatures of 35, 45 and 55 °C was 0.95, 0.92 and 0.72, respectively.

Table 2 lists the OTR values through the PP cap and PET body to various bottle regions at various

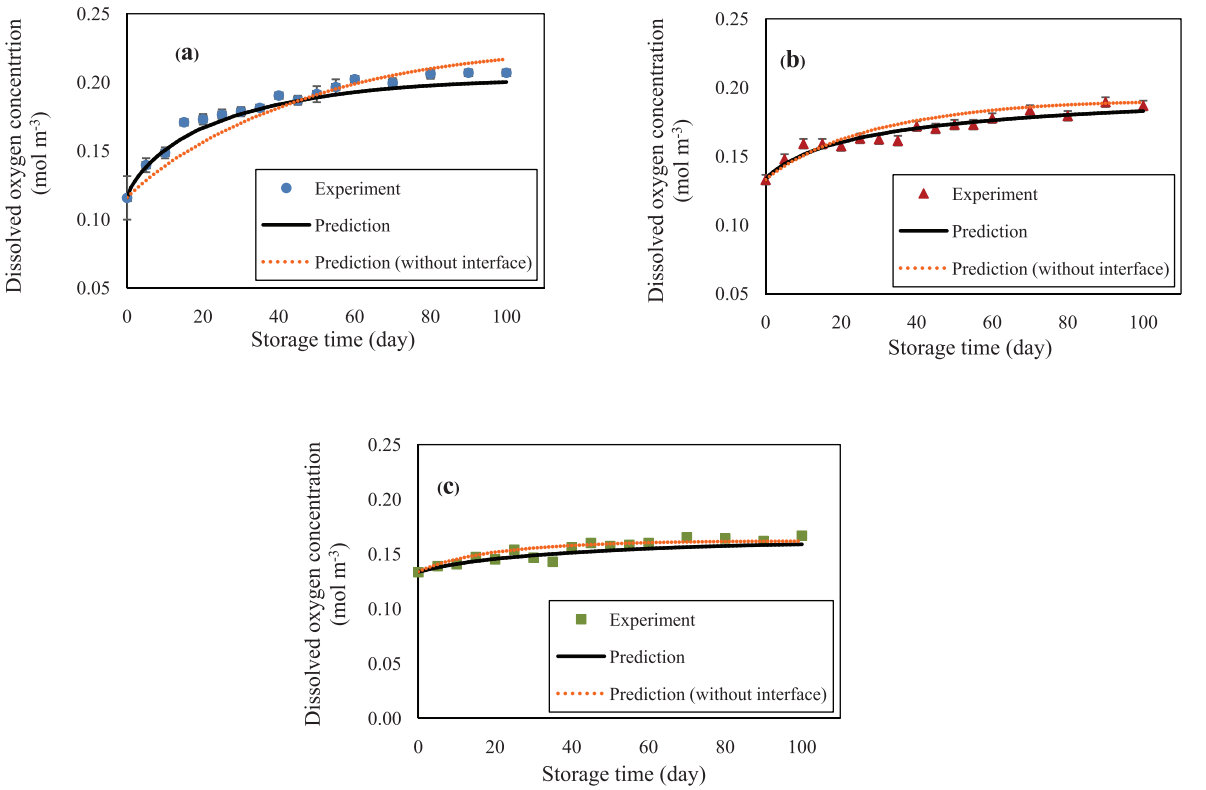

Figure 7 Experimental and predicted dissolved oxygen concentration evolutions at (a) 35 °C; (b) 45 °C and (c) 55 °C with and without considering headspace-water interface

storage temperatures. OTR was calculated from the simulated fluxes of oxygen during the first 20 storage days since OTR reached the maximum values by the end of such a period at all storage conditions. The results expectedly indicated that an increase in the storage temperature led to a higher OTR to the headspace region. This is because the oxygen permeabilities of both PP and PET are higher at a higher temperature. OTR through the PP cap was higher than that through the PET body due to the higher oxygen permeability of the former (see Table 1).

Fig. 8 shows the plots of the fractions of oxygen transported through PP cap and PET body at different storage temperatures. Generally, OTR is calculated as the rate per unit surface area of a packaging. Fig. 8 thus shows that as much as 97-99% of the oxygen transport was through the PP cap. On the other hand, when the total OTR was calculated without dividing the rate by the surface

area, the oxygen transport through the PP cap was around 90-96%, which was slightly lower. This is because the surface area of the PET body of the headspace region (3.43×10^{-3} m^2) is about 4 times larger than that of the PP cap (8.55×10^{-4} m^2).

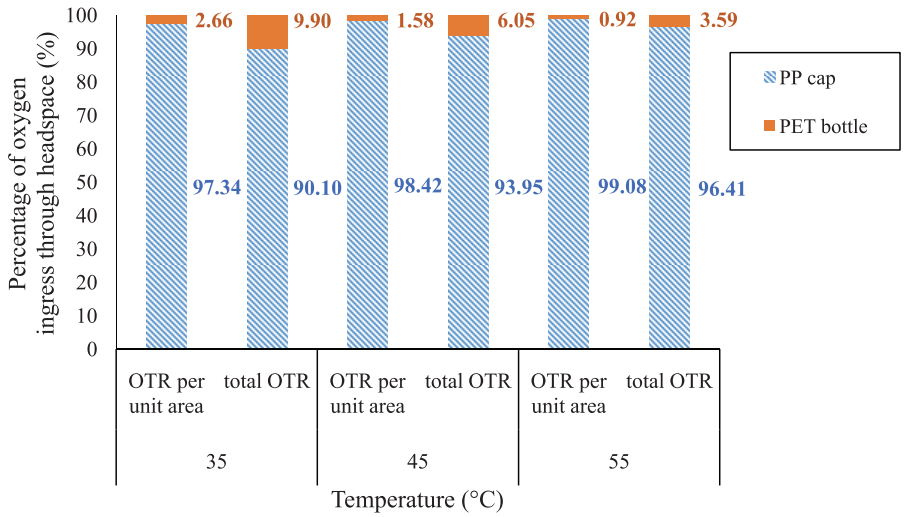

Figure 8 Percentage of oxygen transport through different routes into headspace at different storage temperatures as calculated from OTR per unit area of different routes and total OTR (not per unit area)

In the case of oxygen transport to the water region, an increase in the storage temperature resulted in a lower OTR. This is again because the solubility of oxygen in the water is lower at a higher temperature [13], leading to the lower oxygen migration (or flux) from the surrounding into the water. Oxygen migration through the headspace-water interface was, on the other hand, noted to be higher at a higher storage temperature. Note that the oxygen transport through the headspace-water interface is a function of the partial pressure of oxygen in the headspace region as well as the oxygen solubility in the water as dictated by the Henry's law. When the partial pressure of oxygen in the headspace region increased, although the oxygen solubility in the water decreased, the dissolved oxygen concentration increased. This implies that the oxygen concentration in the headspace region plays a more influential role in this case than the oxygen solubility in the water.

The fractions of oxygen transported through the headspace-water interface and the PET bottle body of the water region are shown in Fig. 9. If the results were considered in terms of the OTR per unit area, oxygen would mostly transport through the headspace-water interface (around 59-85%) and not the PET body of the water region. Since different transport routes have different areas, to make the results more realistic, the fractions should be compared in terms of the total OTR. The transport area of the PET body is larger than that of the headspace-water interface by around 18 times, resulting in as much as 73-92% oxygen transport via the PET body to the water region. The results

here showed that the analysis method of most other previous studies may result in a misunderstanding of the behavior of oxygen transport through various parts of a bottle.

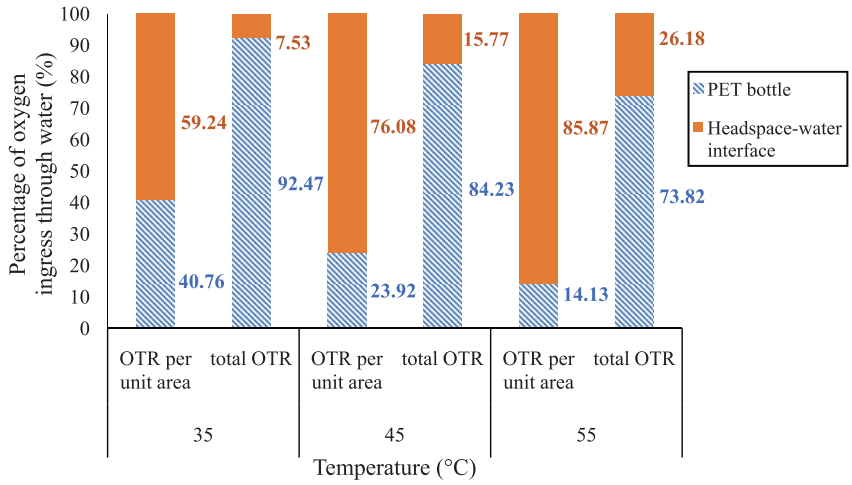

Figure 9 Percentage of oxygen transport through different routes into water at different storage temperatures as calculated from OTR per unit area of different routes and total OTR (not per unit area)

4.4 Simulated effect of selected parameters on dissolved oxygen concentration

The validated model was used to study the effects of bottle thickness and cap material on the evolution of the dissolved oxygen concentration during 100-day storage at a fixed storage temperature of 35 °C. This temperature was selected as it was the temperature that led to the most obvious change in the dissolved oxygen concentration.

4.4.1 Effect of bottle thickness

Fig. 10 shows the evolutions of the dissolved oxygen concentration when various bottle thickness values (0.1-0.3 mm) were used. Note that the thickness of a typical commercial bottle is 0.3 mm. As expected, when the bottle thickness decreased from 0.3 mm to 0.1 mm, the dissolved oxygen concentration increased more rapidly. This is because the oxygen molecules could more easily transport through the thinner bottle wall. The maximum OTR within the first 20 days of storage was noted to be all within the higher oxygen barrier range according to the classification of Abdellatief and Welt [22]. However, when the present results were applied to the data of Kennedy et al. [23] and Roig et al. [24] who studied the effect of dissolved oxygen concentration on ascorbic acid degradation in orange juice, it was found that the bottle thickness would affect the product shelf life. The shelf life of orange juice packed in the bottle with the thickness of 0.3 mm was predicted to be around 41 days, while those packed in the bottles with the thickness of 0.2 and 0.1 mm were predicted to be 38 and 30 days, respectively. These shelf life calculations were based on the recommended minimum ascorbic acid concentration of orange juice of 200 mg L^{-1} [25-28]. The results indicated that the slight change of the OTR has a significant effect on the beverage quality. Selection of the bottle thickness must therefore be made with care.

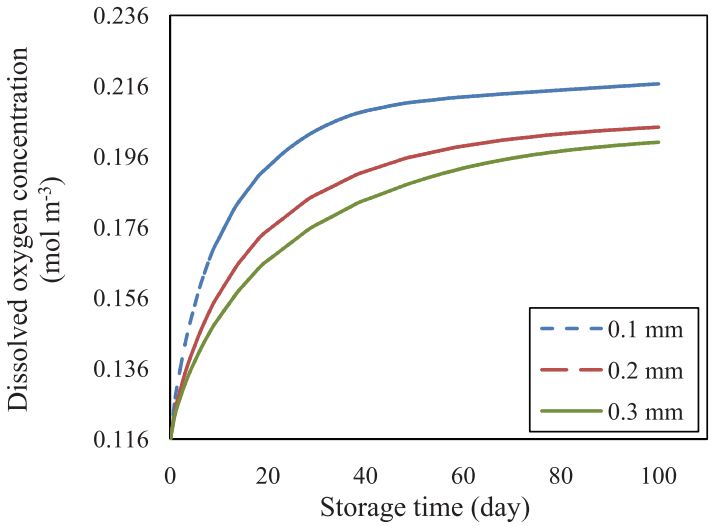

Figure 10 Simulated dissolved oxygen concentration evolutions when using different bottle thickness values

4.4.2 Effect of cap material

PP and PET were tested as the cap materials. Fig. 11 shows that the dissolved oxygen concentration was slightly lower (around 4%) as the cap material was changed from PP to PET, especially when the storage time was beyond 20 days. This is because diffusion is a rather slow process; it took quite some time for the oxygen to transport from the headspace through the headspace-water interface into the water. However, since oxygen migrates through the PP cap faster than through the PET cap, slight change was observed. Therefore, the cap material has no significant effect on the dissolved oxygen concentration if a beverage is to be stored for less than 20 days.

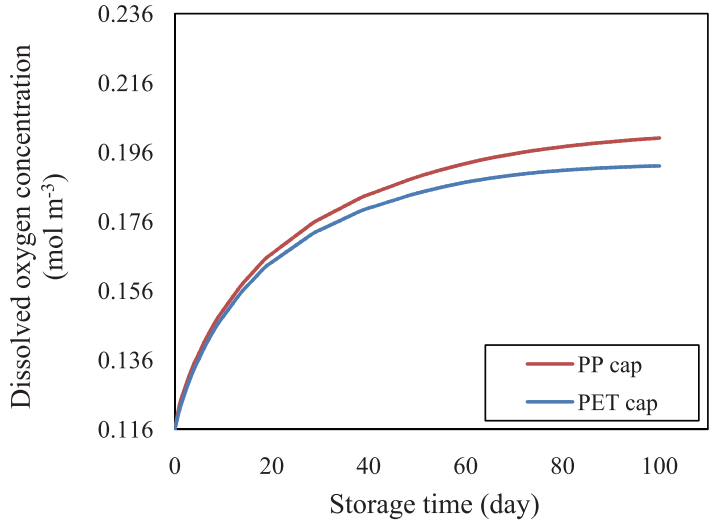

Figure 11 Simulated dissolved oxygen concentration evolutions when using different cap materials

5. Conclusions

A mathematical model based on Fick's law of diffusion was used in conjunction with Henry's law to investigate the oxygen transport though various parts of a PET bottle (bottle body and cap) containing water stored at different temperatures. The model was able to well predict the oxygen concentration evolutions both in the headspace and water regions. Oxygen transport through the cap and headspace-water interface was noted to be significant and must be taken into consideration to arrive at the realistic results. Oxygen mostly transported through the PP cap (around 90-96%) into the headspace region and through the PET body (around 73-92%) into the water region. Although OTR through the headspace-water interface was 59-85% higher than that through the PET body of the water region, 73-92% of the oxygen transported into the water was through the PET body since the headspace-water interface area is much smaller. Analyzing the oxygen transport data as OTR per unit transport area may indeed result in a misunderstanding behavior of oxygen transport through various parts of a bottle. Simulation also showed that bottle thickness significantly affected the dissolved oxygen concentration; increase in the concentration may in turn significantly affect the beverage quality. Cap material, on the other hand, did not pose any significant effect on the dissolved oxygen concentration, especially during the first 20 days of storage.

However, the study did not include the effect of oxygen absorption on the packaging material prior to being transported into the headspace or water. Moreover, the model should be enhanced to allow the prediction of the oxygen transport into a bottle containing an oxygen-sensitive beverage. Since oxygen is an important factor affecting the quality of food through such routes as oxidation reactions, deterioration of food quality during storage should be modeled.

6. Acknowledgements

The authors express their sincere appreciation to the Thailand Research Fund (TRF, Grant number RTA 5880009) as well as the Food and Drug Administration of Thailand for supporting the study financially. The authors are also grateful to T.C. Pharmaceutical Industries Co., Ltd., for its support with the production of bottled water as well as for allowing the use of some laboratory facilities. Author Kaewboonruang thanks the Petchra Pra Jom Klao Scholarship of King Mongkut's University of Technology Thonburi for supporting her master's study.

7. References

1. Adoua, R., Mietton-Peuchot, M. and Milisic, V., 2010, "Modeling of Oxygen Transfer in Wines," *Chemical Engineering Science*, 65, pp. 5455-5463.

2. Dombre, C., Rigou, P., Wirth, J. and Chalier, P., 2015, "Aromatic Evolution of Wine Packed in Virgin and Recycled PET Bottles," *Food Chemistry*, 176, pp. 376-387.

3. Bacigalupi, C., Maurey, A., Boutroy, N., Peyron, S., Avallone, S. and Chalier, P., 2016, "Changes in Nutritional Value of a Multi-vitamins Fortified Juice Packed in Glass and Standard PET Bottles," *Food Control*, 60, pp. 256-262.

4. Chaix, E., Guillaume, C., Gontard, N. and Guillard, V., 2016, "Performance of a Non-invasive Methodology for Assessing Oxygen Diffusion in Liquid and Solid Food Products," *Journal of Food Engineering*, 171, pp. 87-94.

5. Mastromatteo, M. and Del Nobile, M.A., 2011, "A Simple Model to Predict the Oxygen Transport Properties of Multilayer Films," *Journal of Food Engineering*, 102, pp. 170-176.

6. Siracusa, V., 2012, "Food Packaging Permeability Behavior: A Report," *International Journal of Polymer Science*, pp. 1-11.

7. Di Felice, R., Cazzola, D., Cobror, S. and

Oriani, L., 2008, "Oxygen Permeation in PET Bottles with Passive and Active Walls," *Packaging Technology and Science*, 21, pp. 405-415.

8. Van Bree, I., Meulenaer, B.D., Samapundo, S., Vermeulen, A., Ragaert, P., Maes, K.C., Baets, B.D. and Devlieghere, F., 2010, "Predicting the Headspace Oxygen Level due to Oxygen Permeation Across Multilayer Polymer Packaging Materials: A Practical Software Simulation Tool," *Innovative Food Science and Emerging Technologies*, 11, pp. 511-519.

9. Bacigalupi, C., Lemaistre, M.H., Boutroy, N., Bunel, C., Peyron, S., Guillard, V. and Chalier, P., 2013, "Changes in Nutritional and Sensory Properties of Orange Juice Packed in PET Bottles: An Experimental and Modeling Approach,"*Food Chemistry*, 141, pp. 3827-3836.

10. Ballance, R., 1996, "Field Testing Methods," pp. 95-111, in J. Bartram and R. Ballance (Eds.), *Water Quality Monitoring: A Practical Guide to the Design and Implementation of Freshwater Quality Studies and Monitoring Programmes*, E & FN Spon, London.

11. McKeen, L.W., 2012, Permeability Properties of Plastics and Elastomers, 3rd ed., William Andrew, Waltham.

12. Penicaud, C., Broyart, B., Peyron, S., Gontard, N. and Guillard, V., 2011, "Mechanistic Model to Couple Oxygen Transfer with Ascorbic Acid Oxidation Kinetics in Model Solid Food," *Journal of Food Engineering*, 104, pp. 96-104.

13. Sander, R., 2015, "Compilation of Henry's Law Constants (version 4.0) for Water as Solvent," *Atmospheric Chemistry and Physics*, 15, pp. 4399-4981.

14. Bird, R.B., Stewart, W.E. and Lightfoot, E.N., 2002, Transport Phenomena, 2nd ed., Wiley, New York.

15. Geankoplis, C.J., 1993, Transport Processes and Unit Operations, 3rd ed., Prentice Hall, Upper Saddle River.

16. Dincer, I. and Rosen, M., 2002, Thermal Energy Storage: Systems and Applications, Wiley, New York.

17. Denny, M.W., 1993, Air and Water: The Biology and Physics of Life's Media, Princeton University Press, Princeton.

18. Schmid, M., Müller, K., Sängerlaub, S., Huber, C. and Fritsch, K., 2012, "Temperature-dependent Oxygen Permeation through PET/MXD6-barrier Blend Bottles with and without Oxygen Absorber,"*The 5th International Symposium on Food Packaging*, 14-16 November 2012, Berlin, pp. 161-167.

19. Izagirre, O., Bermejo, M., Pozo, J. and Elosegi, A., 2007, "Rivermet: An Excel-based Tool to Calculate River Metabolism from Diel Oxygen-concentration Curves," *Environmental Modeling and Software*, 22, pp. 24-32.

20. Tromans, D., 1998, "Temperature and Pressure Dependent Solubility of Oxygen in Water: A Thermodynamic Analysis," *Hydrometallurgy*, 48, pp. 327-342.

21. Roig, M.G., Bello, J.F., Rivera, Z.S. and Kennedy, J.F., 1994, "Possible Additive for Extension of Shelf-life of Single-strength Reconstituted Citrus Juice Aseptically Packaged in Laminated Cartons," *International Journal of Food Science and Nutrition*, 45, pp. 15-28.

22. Abdellatief, A. and Welt, B.A., 2012, "Comparison of New Dynamic Accumulation Method for Measuring Oxygen Transmission Rate of Packaging against the Steady-state Method Described by ASTM D3985," *Packaging Technology and Science*, 26, pp. 281-288.

23. Kennedy, J.F., Rivera, Z.S., Lloyd, L.L., Warner, F.P. and Jumel, K., 1992, "L-ascorbic acid Stability in Aseptically Processed Orange Juice in TetraBrik Cartons and the Effect of Oxygen,"*Food Chemistry*, 45, pp. 327-331.

24. Roig, M.G., Bello, J.F., Rivera, Z.S. and

Kennedy, J.F., 1999, "Studies on the Occurrence of Non-enzymatic Browning during Storage of Citrus Juice," *Food Research International*, 32, pp. 609-619.

25. Polydera, A.C., Stoforos, N.G. and Taoukis, P.S., 2003, "Comparative Shelf Life Study and Vitamin C Loss Kinetics in Pasteurised and High Pressure Processed Reconstituted Orange Juice," *Journal of Food Engineering*, 60, pp. 21-29.

26. Berlinet, C., Brat, P., Brillouet, J.M. and Ducruet, V., 2006, "Ascorbic Acid, Aroma Compounds and Browning of Orange Juices Related to PET Packaging Materials and pH," *Journal of the Science of Food and Agriculture*, 86, pp. 2206-2212.

27. Ros-Chumillas, M., Belissario, Y., Iguaz, A. and Lopez, A., 2007, "Quality and Shelf Life of Orange Juice Aseptically Packaged in PET Bottles," *Journal of Food Engineering*, 79, pp. 234-242.

28. Wibowo, S., Grauwet, T., Santiago, .S., Tomic, J., Vervoort, L., Hendrickx, M. and Van Loey, A., 2015, "Quality Changes of Pasteurized Orange Juice during Storage: A Kinetic Study of Specific Parameters and their Relation to Colour Instability," *Food Chemistry*, 187, pp. 140-151.